

LNK/*SH2B3* as a novel driver in juvenile myelomonocytic leukemia

Astrid Wintering,¹ Anna Hecht,² Julia Meyer,¹ Eric B. Wong,¹ Juwita Hübner,¹ Sydney Abelson,¹ Kira Feldman,¹ Vanessa E. Kennedy,³ Cheryl A.C. Peretz,^{1,4} Deborah L. French,⁵ Jean Ann Maguire,⁵ Chintan Jobaliya,⁵ Marta Rojas Vasquez,⁶ Sunil Desai,⁶ Robin Dulman,⁷ Eneida Nemecek,⁸ Hilary Haines,⁹ Mahmoud Hammad,¹⁰ Alaa El Haddad,¹⁰ Scott C. Kogan,¹¹ Zied Abdullaev,¹² Farid F. Chehab,¹³ Sarah K. Tasian,^{14,15} Catherine C. Smith,^{3,4} Mignon L. Loh^{16#} and Elliot Stieglitz^{1,4#}

¹Department of Pediatrics, Benioff Children's Hospital, University of California San Francisco, San Francisco, CA, USA; ²Department of Hematology/Oncology, Technical University of Munich, Munich, Germany; ³Division of Hematology/Oncology, Department of Medicine, University of California San Francisco, San Francisco, CA, USA; ⁴Helen Diller Comprehensive Cancer Center, University of California San Francisco, San Francisco, CA, USA; ⁵Center for Cellular and Molecular Therapeutics, The Children's Hospital of Philadelphia, Philadelphia, PA, USA; ⁶Department of Pediatrics, University of Alberta, Edmonton, Canada; ⁷Pediatric Hematology and Oncology, Pediatric Specialists of Virginia, Fairfax, VA, USA; ⁸OHSU Knight Cancer Institute, Oregon Health and Science University, Portland, OR, USA; ⁹Children's of Alabama, University of Alabama Hospital, Birmingham, AL, USA; ¹⁰National Cancer Institute, Cairo University, Cairo, Egypt; ¹¹Department of Laboratory Medicine, University of California San Francisco, San Francisco, CA, USA; ¹²Laboratory of Pathology, Center for Cancer Research, National Cancer Institute, National Institutes of Health, Bethesda, MD, USA; ¹³Institute for Human Genetics, University of California San Francisco, San Francisco, CA, USA; ¹⁴Division of Oncology and Center for Childhood Cancer Research, Children's Hospital of Philadelphia, Philadelphia, PA, USA; ¹⁵Department of Pediatrics and Abramson Cancer Center, University of Pennsylvania Perelman School of Medicine, Philadelphia, PA, USA and ¹⁶Ben Towne Center for Childhood Cancer Research, Seattle Children's Research Institute, and the Department of Pediatrics, Seattle Children's Hospital, University of Washington, Seattle, WA, USA

#MLL and ES contributed equally as senior authors.

Correspondence: E. Stieglitz
elliott.stieglitz@ucsf.edu

M. Loh
mignon.loh@seattlechildrens.org

Received: June 21, 2023.

Accepted: December 19, 2023.

Early view: December 28, 2023.

<https://doi.org/10.3324/haematol.2023.283776>

©2024 Ferrata Storti Foundation

Published under a CC BY-NC license



Supplemental Material

Supplemental Methods

Germline validation

To investigate the germline nature of the *SH2B3* mutation in patients UPN1744 and UPN3436 (Table 1) genomic DNA was isolated from CD3+ sorted T cells and buccal swabs, respectively. Genomic DNA was isolated and purified using the AllPrep DNA/RNA Mini kit (Qiagen) according to directions and 50-100ng of DNA used for exon specific PCR. For UPN1744, *SH2B3* exon 3 primers: F (TGGACCTCACTACAGGCTCA) and R (AATTCAGCTGCTGCTCGTCT) were used and product was Sanger sequenced. For UPN3436, *SH2B3* exon 6 primers: F (TAGCTAGGCCATTGTCTTCTGG) and R (CACGACCGAGGGAAAGTGG) were used and product was Sanger sequenced. Sanger sequences are depicted in Supplemental Figure 2.

Differentiation of iPSC to HPC

Monolayer differentiation of iPSC into HPCs was started when cells were ~70% confluent and was performed as previously described¹. In short, different base medias and cytokines (all growth factor reagents from R&D Systems) were added to promote HPC formation:

Days	Medium	BMP-4	VEGF	CHIR*	bFGF	SCF	Flt3L
0-1	RPMI	5	50	0.5-1.0			
2-3	RPMI/SP34	5	50		20		
4-5	SP34		15		5		
6	SFD		50		100	50	25
7-10	SFD		50		100	50	25

*CHIR concentration in μM ; all other concentrations in ng/mL

All base media were supplemented with L-glutamine (2mM), penicillin/streptomycin (1x), MTG (3 $\mu\text{L/mL}$ of a 26 μL in 2ML IMDM stock) and ascorbic acid (50 $\mu\text{g/mL}$).

HPCs were then collected on day 9 or day 10 of monolayer differentiation and analyzed using flow cytometry (CD41, CD42b, CD235, CD34 and CD45; all antibodies were purchased from BioLegend).

Single-cell DNA and Protein Sample Preparation, Library Generation, and Sequencing

We performed single-cell DNA plus antibody sequencing (DAb-seq) on unsorted mononuclear cells using a microfluidic approach with molecular barcode technology using the Tapestry platform (MissionBio) as previously described^{2,3}. Briefly, cryopreserved cells were thawed and normalized to 10,000 cells/ μL in 180 μL PBS (Corning). Pooled samples were resuspended in cell buffer (MissionBio), diluted to 4-7e6 cells/mL, and then loaded onto a microfluidics cartridge, where individual cells were encapsulated, lysed, and barcoded using the Tapestry instrument. DNA from barcoded cells was amplified via PCR using a targeted panel that included 288 amplicons across 66 genes associated with acute leukemia (Supplemental Table 5). DNA PCR products were isolated, purified with AmpureXP beads (Beckman Coulter), used as a PCR template for library generation, and then repurified with AmpureXP beads. The DNA library was quantified and assessed for quality via a Qubit fluorometer (Life Technologies) and Bioanalyzer (Agilent Technologies) prior to pooling for sequencing on an Illumina Novaseq.

Single-Cell DAb-seq Data Processing and Analysis

FASTQ files were processed via an open-source pipeline as described previously². This analysis pipeline trims adaptor sequences, demultiplexes DNA panel amplicons and antibody tags into single cells, and aligns panel reads to the hg19 reference genome. Valid cell barcodes were called using the inflection point of the cell-rank plot in addition to the requirement that 60% of DNA intervals were covered by at least eight reads. Variants were called using GATK (v 4.1.3.0) according to GATK best practices⁴. For each valid cell barcode, variants were filtered according to quality and sequence depth reported by GATK, with low quality variants and cells excluded based on the cutoffs of quality score < 30, read depth < 10, and alternate allele frequency < 20%. We analyzed all variants present in >0.1% of cells. Variants were assessed for known or likely pathogenicity via ClinVar and COSMIC databases^{5,6}, and previously identified, non-intronic somatic variants were included in clonal analyses, as per prior single cell DNA (SC DNA) studies^{7,8}. The patient's phylogenetic tree was inferred using single cell inference of tumor evolution (SCITE), a probabilistic model using a flexible Markov-chain Monte Carlo algorithm⁹. SCITE was employed with a global false positive rate set to 1% and a platform-provided false-negative rate, as per prior SC DNA studies⁸. Only cells with complete genotyping of variants of interest, as identified via prior bulk sequencing, were included in phylogenetic analysis.

Supplemental Case Vignette

Case Vignette - UPN2823

A 6-year-old boy presented with 12% peripheral myeloblasts and elevated age-adjusted fetal hemoglobin. Abdominal ultrasound demonstrated splenomegaly.

Cytogenetic and FISH analysis were normal. DNA sequencing detected two mutations in SH2B3 p.R308 (VAF 46%) and p.G225fs*47 (VAF 21%), a mutation in RRAS2 p.Q72L (VAF 40%), a mutation in ZRSR2 p.Q255* (VAF 19%), and a PTPN11 p.T73I mutation (VAF 4%). A buccal sample was negative for all of the above mutations. Five months after diagnosis, he received allogeneic HCT from a 10/10 human leukocyte antigen-matched unrelated donor after conditioning with busulfan, cyclophosphamide, and melphalan. Following transplant, the patient developed both acute and chronic graft versus host disease (GvHD) with bronchiolitis obliterans. The patient is still receiving pulmonary therapy but does not require supplemental oxygen and currently has no signs of disease three years post-transplant.*

Supplemental Tables

Supplemental Table 1: Overview of iPSC lines used in this study

Patient Sample ID	Cell Source	Reprogramming Vector	Driver Mutation		Secondary Mutation	
			Gene	Mutation	Gene	Mutation
UPN3037	BM	Sendai	PTPN11	+/+	-	-
				p.E69K/+	-	-
					SH2B3	p.W262X p.H414Y

Supplemental Table 2: List of the top 10 compounds that showed a greater inhibition of *PTPN11*/*SH2B3* double mutant HPCs than of *PTPN11* single mutant HPCs.

#	Drug	Target	Pathway
1	Adavosertib (MK-1775)	Wee1	Cell Cycle
2	Givinostat (ITF2357)	HDAC	Cytoskeletal Signaling
3	CEP-33779	JAK	JAK/STAT
4	CUDC-101	EGFR, HDAC, HER2	Epigenetics
5	AT9283	Aurora Kinase, Bcr-Abl, JAK	JAK/STAT
6	Abexinostat (PCI-24781)	HDAC	Cytoskeletal Signaling
7	Momelotinib (CYT387)	JAK	JAK/STAT
8	Nexturastat A	HDAC	DNA Damage
9	Milciclib (PHA-848125)	CDK	Cell Cycle
10	M344	HDAC	Cytoskeletal Signaling

Supplemental Table 3: Frequencies of subclones of UPN2861 identified by single-cell sequencing.

Clone	Number of Mutated Single Cells (%)
<i>SH2B3</i> + <i>PTPN11</i> + <i>IKZF1</i>	20 (8.9%)
<i>SH2B3</i> + <i>PTPN11</i> + <i>WT1</i>	31 (13.9%)
<i>SH2B3</i> + <i>PTPN11</i>	143 (63.2%)
<i>SH2B3</i>	3 (1.3%)
<i>SH2B3</i> - Homozygous	4 (1.8%)
No detectable pathogenic mutations	22 (9.9%)

Supplemental Table 4: Previously reported patients with *SH2B3* alterations¹¹.

Case ID	Sex	Age at diagnosis	<i>SH2B3</i> alteration (VAF%)	Configuration of <i>SH2B3</i> alteration	Additional alterations	Cytogenetic abnormalities	Treatment	Outcome
UPN1420	M	2y	p.F390fs (42%); p.Q258* (25%)	Somatic	<i>NF1</i> p.Y2285* (46%); <i>NF1</i> p.I679fs (38%); <i>ASXL1</i> p.Y591* (51%)	No	HCT	Deceased
UPN2531	M	3y	p.W262* (35%); p.H414fs (40%)	Somatic	<i>PTPN11</i> p.E69K (39%)	No	HCT	Deceased
UPN1970	F	7m	p.E400K (43%)	Germline	None	No	HCT	Alive
J295	M	2.5y	p.T419fs (58%)	n/a	<i>PTPN11</i> p.E76K (46%)	n/a	n/a	Deceased
J316	M	4.6y	p.F431fs (34%)	n/a	<i>PTPN11</i> p.G503A (63%); <i>RRAS</i> p.R132H (46%)	n/a	Chemotherapy	Deceased
J322	M	4.2y	p.R261W (10%)	n/a	<i>PTPN11</i> p.D61V (52%); <i>NF1</i> p.R440* (24%); <i>NF1</i> p.R1306* (13%)	n/a	HCT	Alive
J325	M	4y	p.Q72H (17%)	n/a	None	n/a	n/a	Deceased

Supplemental Table 5: Amplicon panel used for single cell sequencing.

Chromosome	Gene	Amplicon start	Amplicon end
chr1	<i>PIK3CD</i>	9775671	9775941
chr1	<i>PIK3CD</i>	9781387	9781645
chr1	<i>PIK3CD</i>	9782105	9782371
chr1	<i>PIK3CD</i>	9782490	9782702
chr1	<i>PIK3CD</i>	9783227	9783486
chr1	<i>PIK3CD</i>	9784116	9784376
chr1	<i>PIK3CD</i>	9786999	9787257
chr1	<i>CSF3R</i>	36933146	36933346
chr1	<i>CSF3R</i>	36933346	36933606
chr1	<i>MACF1</i>	39723577	39723814
chr1	<i>NRAS</i>	115256487	115256723
chr1	<i>NRAS</i>	115258609	115258825
chr1	<i>RIT1</i>	155880253	155880493
chr10	<i>SMC3</i>	112343860	112344065
chr10	<i>SMC3</i>	112356141	112356380
chr10	<i>SMC3</i>	112360272	112360528
chr10	<i>SHOC2</i>	112723994	112724234
chr11	<i>HRAS</i>	534082	534333
chr11	<i>RRAS2</i>	14316323	14316546
chr11	<i>WT1</i>	32410614	32410840
chr11	<i>WT1</i>	32413427	32413633
chr11	<i>WT1</i>	32414189	32414405
chr11	<i>WT1</i>	32439082	32439321

chr11	<i>WT1</i>	32449937	32450197
chr11	<i>WT1</i>	32456240	32456481
chr11	<i>KMT2A</i>	118368522	118368745
chr11	<i>CBL</i>	119142363	119142580
chr11	<i>CBL</i>	119148869	119149075
chr11	<i>CBL</i>	119149076	119149333
chr11	<i>CBL</i>	119149338	119149575
chr11	<i>CBL</i>	119168935	119169145
chr11	<i>CBL</i>	119170258	119170486
chr12	<i>KDM5A</i>	420042	420282
chr12	<i>KDM5A</i>	430179	430396
chr12	<i>KDM5A</i>	443425	443663
chr12	<i>ETV6</i>	11992084	11992315
chr12	<i>ETV6</i>	12006322	12006542
chr12	<i>ETV6</i>	12022379	12022639
chr12	<i>ETV6</i>	12022749	12023009
chr12	<i>ETV6</i>	12043767	12043994
chr12	<i>KRAS</i>	25378535	25378795
chr12	<i>KRAS</i>	25380238	25380478
chr12	<i>KRAS</i>	25398227	25398433
chr12	<i>SH2B3</i>	111884535	111884777
chr12	<i>SH2B3</i>	111884791	111885049
chr12	<i>SH2B3</i>	111885214	111885424
chr12	<i>PTPN11</i>	112884014	112884254
chr12	<i>PTPN11</i>	112888115	112888350
chr12	<i>PTPN11</i>	112893742	112893975
chr12	<i>PTPN11</i>	112915377	112915582
chr12	<i>PTPN11</i>	112926203	112926424
chr12	<i>PTPN11</i>	112926824	112927050
chr12	<i>PTPN11</i>	112942491	112942728
chr13	<i>FLT3</i>	28578139	28578348
chr13	<i>FLT3</i>	28588513	28588753
chr13	<i>FLT3</i>	28589224	28589443
chr13	<i>FLT3</i>	28589621	28589866
chr13	<i>FLT3</i>	28592473	28592726
chr13	<i>FLT3</i>	28597387	28597639
chr13	<i>FLT3</i>	28598932	28599132
chr13	<i>FLT3</i>	28601175	28601423
chr13	<i>FLT3</i>	28602289	28602513
chr13	<i>FLT3</i>	28607933	28608152
chr13	<i>FLT3</i>	28608168	28608392
chr13	<i>FLT3</i>	28608392	28608635
chr13	<i>FLT3</i>	28609600	28609850

chr13	<i>FLT3</i>	28610014	28610260
chr13	<i>FLT3</i>	28611230	28611480
chr13	<i>FLT3</i>	28622379	28622629
chr13	<i>FLT3</i>	28623491	28623741
chr13	<i>FLT3</i>	28623743	28623993
chr13	<i>FLT3</i>	28624191	28624429
chr13	<i>FLT3</i>	28626645	28626890
chr13	<i>FLT3</i>	28631453	28631699
chr13	<i>FLT3</i>	28635981	28636231
chr13	<i>FLT3</i>	28644552	28644798
chr15	<i>MAP2K1</i>	66727349	66727596
chr15	<i>MAP2K1</i>	66728980	66729220
chr15	<i>MAP2K1</i>	66735593	66735803
chr15	<i>MAP2K1</i>	66774053	66774267
chr15	<i>MAP2K1</i>	66782741	66782973
chr15	<i>IDH2</i>	90631740	90631990
chr16	<i>CREBBP</i>	3779649	3779892
chr16	<i>CREBBP</i>	3823590	3823830
chr16	<i>CREBBP</i>	3832666	3832910
chr16	<i>MAPK3</i>	30128455	30128688
chr16	<i>MAPK3</i>	30129372	30129626
chr16	<i>SRCAP</i>	30718974	30719219
chr16	<i>SRCAP</i>	30723827	30724067
chr17	<i>TP53</i>	7572897	7573129
chr17	<i>TP53</i>	7577071	7577315
chr17	<i>TP53</i>	7577397	7577636
chr17	<i>TP53</i>	7578075	7578315
chr17	<i>TP53</i>	7578363	7578623
chr17	<i>TP53</i>	7579501	7579761
chr17	<i>NF1</i>	29508376	29508636
chr17	<i>NF1</i>	29527958	29528193
chr17	<i>NF1</i>	29533184	29533424
chr17	<i>NF1</i>	29553440	29553700
chr17	<i>NF1</i>	29562707	29562943
chr17	<i>NF1</i>	29667507	29667736
chr17	<i>NF1</i>	29683941	29684174
chr17	<i>STAT5B</i>	40354363	40354581
chr17	<i>STAT5B</i>	40354621	40354863
chr17	<i>STAT5B</i>	40359626	40359871
chr17	<i>STAT5B</i>	40370757	40371014
chr17	<i>STAT5A</i>	40452653	40452905
chr17	<i>STAT5A</i>	40460083	40460306
chr17	<i>STAT5A</i>	40461369	40461629

chr17	<i>STAT3</i>	40469205	40469425
chr17	<i>STAT3</i>	40474337	40474543
chr17	<i>STAT3</i>	40475017	40475260
chr18	<i>SETBP1</i>	42531847	42532089
chr19	<i>MAP2K2</i>	4101010	4101267
chr19	<i>MAP2K2</i>	4102235	4102485
chr19	<i>MAP2K2</i>	4110520	4110769
chr19	<i>MAP2K2</i>	4117506	4117766
chr19	<i>JAK3</i>	17943190	17943409
chr19	<i>JAK3</i>	17945519	17945768
chr19	<i>JAK3</i>	17945926	17946185
chr19	<i>JAK3</i>	17947979	17948219
chr19	<i>JAK3</i>	17954120	17954371
chr19	<i>CEBPA</i>	33792253	33792503
chr19	<i>CEBPA</i>	33793090	33793338
chr19	<i>RRAS</i>	50140143	50140413
chr19	<i>CD33</i>	51728357	51728615
chr2	<i>DNMT3A</i>	25457050	25457294
chr2	<i>DNMT3A</i>	25458480	25458718
chr2	<i>DNMT3A</i>	25463106	25463346
chr2	<i>DNMT3A</i>	25463493	25463717
chr2	<i>DNMT3A</i>	25467415	25467632
chr2	<i>ASXL2</i>	25966895	25967154
chr2	<i>ASXL2</i>	25972624	25972869
chr2	<i>ASXL2</i>	25973036	25973241
chr2	<i>SOS1</i>	39249824	39250056
chr2	<i>SF3B1</i>	198266698	198266913
chr2	<i>SF3B1</i>	198267323	198267549
chr2	<i>IDH1</i>	209113085	209113297
chr20	<i>ASXL1</i>	31017032	31017239
chr20	<i>ASXL1</i>	31020968	31021193
chr20	<i>ASXL1</i>	31022168	31022417
chr20	<i>ASXL1</i>	31022567	31022827
chr20	<i>ASXL1</i>	31022965	31023205
chr21	<i>RUNX1</i>	36231692	36231937
chr21	<i>RUNX1</i>	36252819	36253046
chr21	<i>U2AF1</i>	44514752	44514997
chr21	<i>U2AF1</i>	44524416	44524634
chr22	<i>MAPK1</i>	22127115	22127325
chr22	<i>MAPK1</i>	22142917	22143157
chr22	<i>MAPK1</i>	22153310	22153534
chr22	<i>MAPK1</i>	22160227	22160456
chr22	<i>MAPK1</i>	22161969	22162197

chr22	<i>MAPK1</i>	22221427	22221652
chr22	<i>EP300</i>	41553275	41553494
chr22	<i>EP300</i>	41556594	41556831
chr22	<i>EP300</i>	41574208	41574447
chr3	<i>SETD2</i>	47058395	47058633
chr3	<i>EP300</i>	47103646	47103860
chr3	<i>GATA2</i>	128200077	128200327
chr3	<i>GATA2</i>	128200668	128200928
chr3	<i>GATA2</i>	128202699	128202899
chr3	<i>PIK3CB</i>	138374149	138374377
chr3	<i>PIK3CB</i>	138376488	138376696
chr3	<i>PIK3CB</i>	138409904	138410124
chr3	<i>PIK3CB</i>	138417747	138417988
chr3	<i>PIK3CB</i>	138426083	138426336
chr3	<i>PIK3CA</i>	178916781	178916981
chr3	<i>PIK3CA</i>	178917420	178917667
chr3	<i>PIK3CA</i>	178921356	178921603
chr3	<i>PIK3CA</i>	178922173	178922395
chr3	<i>PIK3CA</i>	178927282	178927490
chr3	<i>PIK3CA</i>	178927903	178928119
chr3	<i>PIK3CA</i>	178936054	178936314
chr3	<i>PIK3CA</i>	178938890	178939112
chr3	<i>PIK3CA</i>	178947706	178947918
chr3	<i>PIK3CA</i>	178948011	178948270
chr3	<i>PIK3CA</i>	178951922	178952192
chr4	<i>KIT</i>	55589655	55589878
chr4	<i>KIT</i>	55593574	55593801
chr4	<i>KIT</i>	55599270	55599486
chr4	<i>TET2</i>	106156708	106156920
chr4	<i>TET2</i>	106157091	106157322
chr4	<i>TET2</i>	106157488	106157694
chr4	<i>TET2</i>	106157812	106158034
chr4	<i>TET2</i>	106180623	106180844
chr4	<i>TET2</i>	106193715	106193955
chr4	<i>TET2</i>	106196119	106196359
chr4	<i>TET2</i>	106196888	106197127
chr4	<i>TET2</i>	106197190	106197405
chr4	<i>FAT1</i>	187517634	187517877
chr4	<i>FAT1</i>	187524540	187524773
chr4	<i>FAT1</i>	187532681	187532911
chr4	<i>FAT1</i>	187535375	187535615
chr4	<i>FAT1</i>	187541581	187541820
chr4	<i>FAT1</i>	187541862	187542102

chr4	<i>FAT1</i>	187629158	187629398
chr4	<i>FAT1</i>	187629962	187630201
chr4	<i>FAT1</i>	187630314	187630542
chr5	<i>APC</i>	112154882	112155088
chr5	<i>APC</i>	112179777	112180031
chr5	<i>NPM1</i>	170832233	170832491
chr5	<i>NPM1</i>	170834648	170834851
chr5	<i>NPM1</i>	170837462	170837704
chr6	<i>CCND3</i>	41905055	41905274
chr7	<i>ABCA13</i>	48411827	48412060
chr7	<i>IKZF1</i>	50450114	50450357
chr7	<i>PIK3CG</i>	106508471	106508724
chr7	<i>PIK3CG</i>	106508781	106509041
chr7	<i>PIK3CG</i>	106509241	106509486
chr7	<i>PIK3CG</i>	106509515	106509775
chr7	<i>PIK3CG</i>	106512941	106513176
chr7	<i>PIK3CG</i>	106523396	106523615
chr7	<i>BRAF</i>	140434357	140434573
chr7	<i>BRAF</i>	140453059	140453266
chr7	<i>BRAF</i>	140477761	140477983
chr7	<i>BRAF</i>	140481366	140481601
chr7	<i>BRAF</i>	140487266	140487476
chr7	<i>BRAF</i>	140501240	140501441
chr7	<i>EZH2</i>	148504738	148504978
chr7	<i>EZH2</i>	148506372	148506589
chr7	<i>EZH2</i>	148507406	148507618
chr7	<i>EZH2</i>	148511032	148511276
chr7	<i>EZH2</i>	148514917	148515124
chr7	<i>EZH2</i>	148523481	148523726
chr7	<i>EZH2</i>	148525653	148525888
chr7	<i>EZH2</i>	148526737	148526948
chr8	<i>RAD21</i>	117859853	117860065
chr8	<i>RAD21</i>	117875360	117875610
chr8	<i>RAD21</i>	117878806	117879014
chr8	<i>MYC</i>	128750640	128750887
chr8	<i>MYC</i>	128751169	128751429
chr8	<i>MYC</i>	128752604	128752810
chr9	<i>JAK2</i>	5073698	5073902
chr9	<i>JAK2</i>	5078303	5078518
chr9	<i>JAK2</i>	5089672	5089888
chrX	<i>ZRSR2</i>	15827260	15827494
chrX	<i>ZRSR2</i>	15833847	15834083
chrX	<i>ZRSR2</i>	15841187	15841437

chrX	<i>BCOR</i>	39911356	39911576
chrX	<i>BCOR</i>	39922077	39922301
chrX	<i>BCOR</i>	39931984	39932228
chrX	<i>BCOR</i>	39933343	39933549
chrX	<i>BCOR</i>	39933743	39934001
chrX	<i>BCOR</i>	39934038	39934256
chrX	<i>STAG2</i>	123171369	123171576
chrX	<i>STAG2</i>	123176321	123176536
chrX	<i>STAG2</i>	123179153	123179393
chrX	<i>STAG2</i>	123181213	123181443
chrX	<i>STAG2</i>	123197003	123197263
chrX	<i>STAG2</i>	123215277	123215534
chrX	<i>STAG2</i>	123220412	123220633
chrX	<i>PHF6</i>	133527460	133527667
chrX	<i>PHF6</i>	133547448	133547683
chrX	<i>PHF6</i>	133549065	133549325
chrX	<i>PHF6</i>	133551195	133551417

Supplemental Figure Legends

Supplemental Figure 1. Photomicrographs were taken of patient diagnostic samples.

Panel A Bone marrow biopsy of UPN3160 showing myeloid hyperplasia (mature and precursors), scattered eosinophils, and few megakaryocytes. *Panel B* Bone marrow aspirate of UPN2861 showing numerous monocytic cells, several neutrophilic cells, and a nucleated red blood cells. *Panel C* Peripheral blood smear of UPN3426 showing mixture of cell types including neutrophil, monocytes, eosinophil precursor, nucleated red blood cell, and blast. *Panel D* Bone marrow aspirate of UPN3426 showing left-shifted granulocyte precursors, increased monocytes, few blasts, and few lymphocytes. *Panel E* Peripheral blood smear of patient UPN3436 showing mixture of cell types including neutrophils (including hypogranular forms), monocytes, eosinophils, basophil, lymphocyte, and nucleated red blood cell. *Panel F* Bone marrow aspirate of UPN3436 showing left-shifted granulocyte precursors, monocytes, few

blasts, few nucleated red >blood cells, and a portion of a megakaryocyte (lower left).
(A: 40X objective, Hematoxylin & Eosin. B – F: 100X objective, Wright-Giemsa.)

Supplemental Figure 2. Sanger sequencing confirms germline configuration of *SH2B3* mutations in UPN1744 (left) and UPN3436 (right).

Supplemental Figure 3. *Panel A* Mutant iPSC-derived HPC but not wildtype HPC show spontaneous proliferation independent of GM-CSF, a hallmark of JMML. *Panel B* Immunoblotting of single and double mutant HPC showed elevated STAT5 and ERK signaling compared to WT HPC.

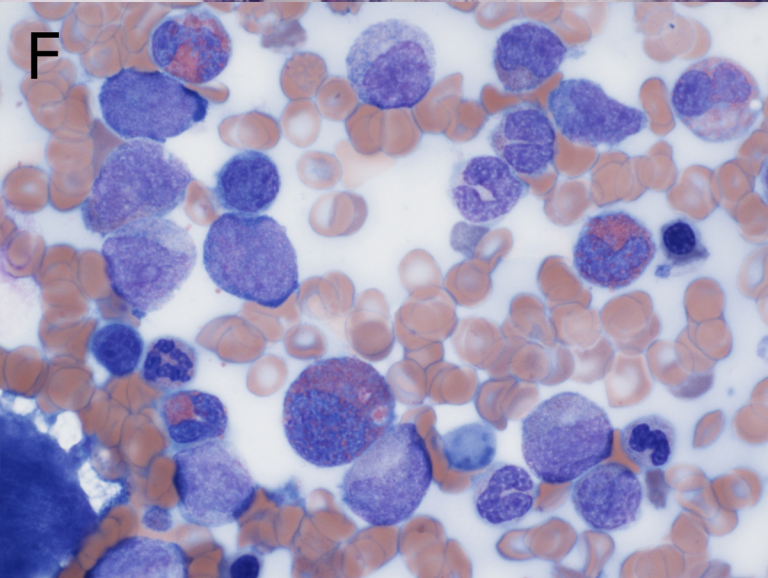
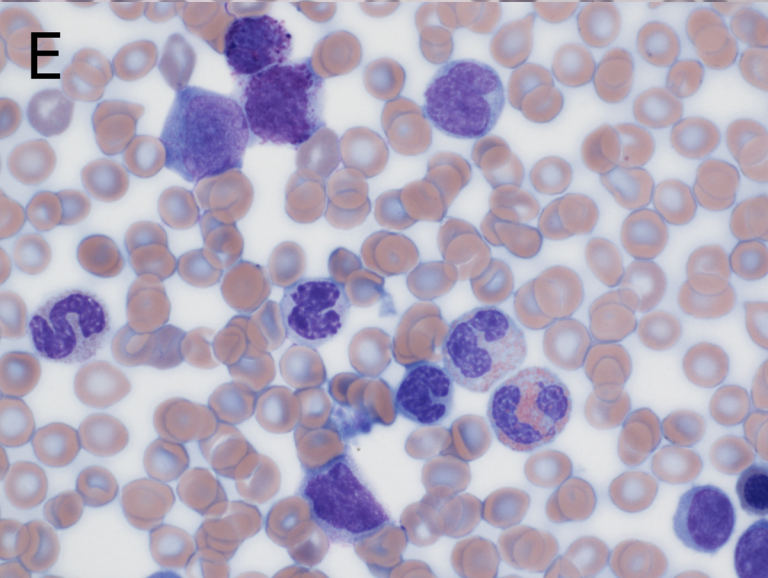
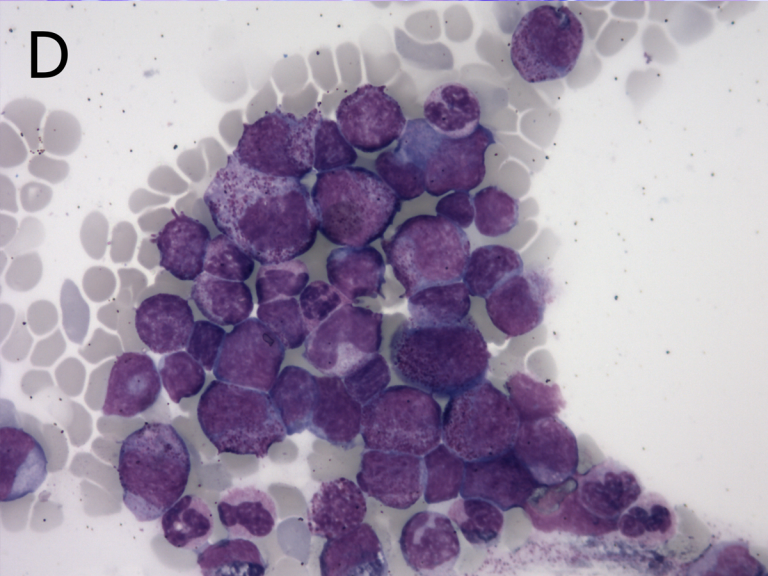
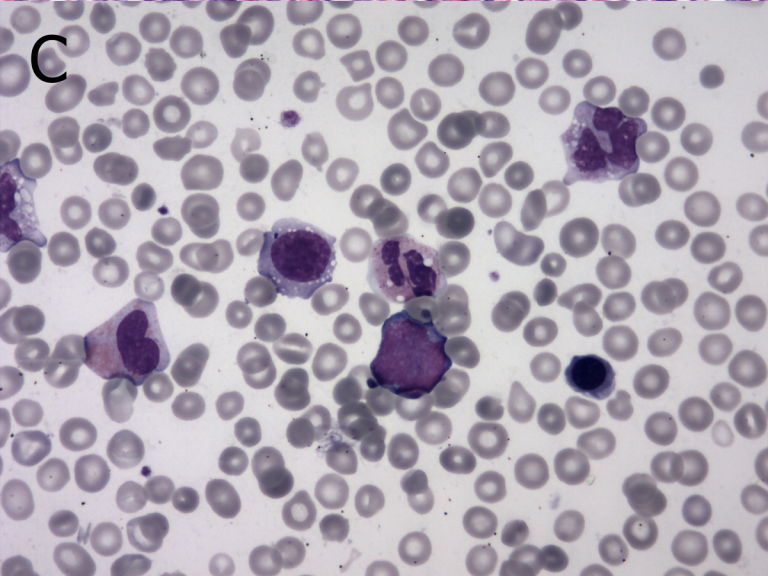
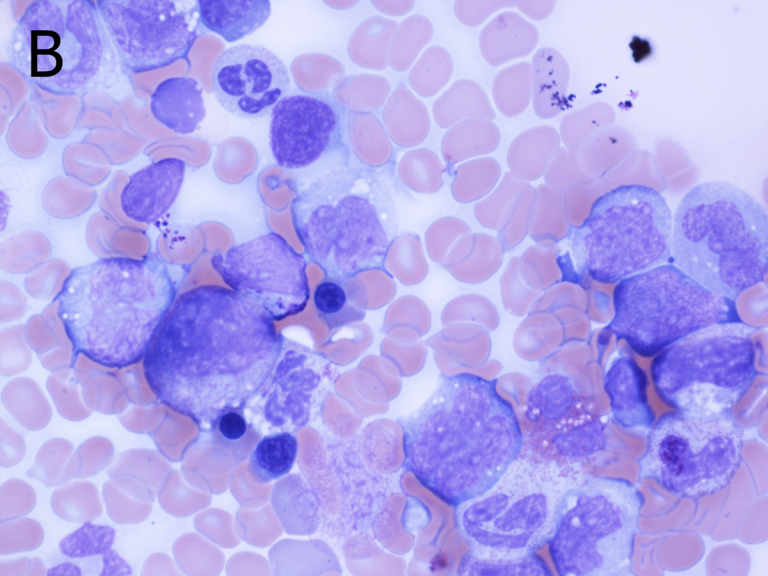
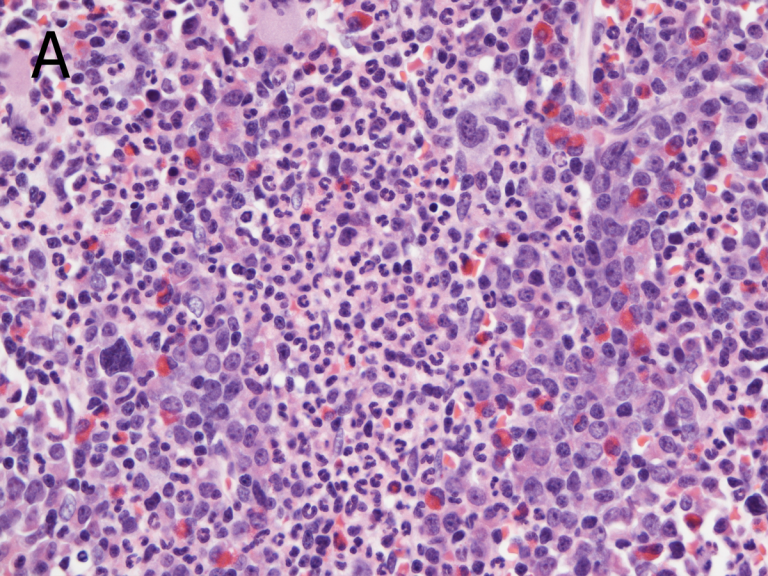
Supplemental Figure 4. Circos plot highlighting the association of *SH2B3* and *PTPN11* alterations. All but one patient with germline *SH2B3* (g_ *SH2B3*) mutation had no additional alterations, while patients with somatic *SH2B3* (s_ *SH2B3*) mutations as well as *SH2B3* mutations of unknown configuration (u_ *SH2B3*) frequently carried additional mutations in *PTPN11* compared to other Ras/MAPK signaling genes.

Supplemental References

1. Mills JA, Paluru P, Weiss MJ, Gadue P, French DL. Hematopoietic Differentiation of Pluripotent Stem Cells in Culture. In: *Methods in Molecular Biology*, vol. 1185. 2014. p181–194.
2. Demaree B, Delley CL, Vasudevan HN, et al. Joint profiling of DNA and proteins in single cells to dissect genotype-phenotype associations in leukemia. *Nat Commun* 2021;12(1):1583.
3. Pellegrino M, Sciambi A, Treusch S, et al. High-throughput single-cell DNA sequencing of acute myeloid leukemia tumors with droplet microfluidics.

Genome Res 2018;28(9):1345–1352.

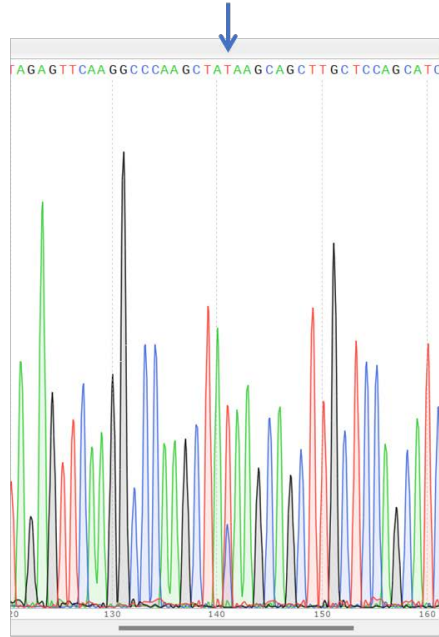
4. DePristo MA, Banks E, Poplin R, et al. A framework for variation discovery and genotyping using next-generation DNA sequencing data. *Nat Genet* 2011;43(5):491–498.
5. Landrum MJ, Lee JM, Benson M, et al. ClinVar: improving access to variant interpretations and supporting evidence. *Nucleic Acids Res* 2018;46(D1):D1062–D1067.
6. Tate JG, Bamford S, Jubb HC, et al. COSMIC: the Catalogue Of Somatic Mutations In Cancer. *Nucleic Acids Res* 2019;47(D1):D941–D947.
7. Miles LA, Bowman RL, Merlinsky TR, et al. Single-cell mutation analysis of clonal evolution in myeloid malignancies. *Nature* 2020;587(7834):477–482.
8. Morita K, Wang F, Jahn K, et al. Clonal evolution of acute myeloid leukemia revealed by high-throughput single-cell genomics. *Nat Commun* 2020;11(1):5327.
9. Jahn K, Kuipers J, Beerenwinkel N. Tree inference for single-cell data. *Genome Biol* 2016;1786.
10. Mulè MP, Martins AJ, Tsang JS. Normalizing and denoising protein expression data from droplet-based single cell profiling. *Nat Commun* 2022;13(1):2099.
11. Stieglitz E, Taylor-Weiner AN, Chang TY, et al. The Genomic Landscape of Juvenile Myelomonocytic Leukemia. *Nat Genet* 2015;47(11):1326–1333.



UPN1744

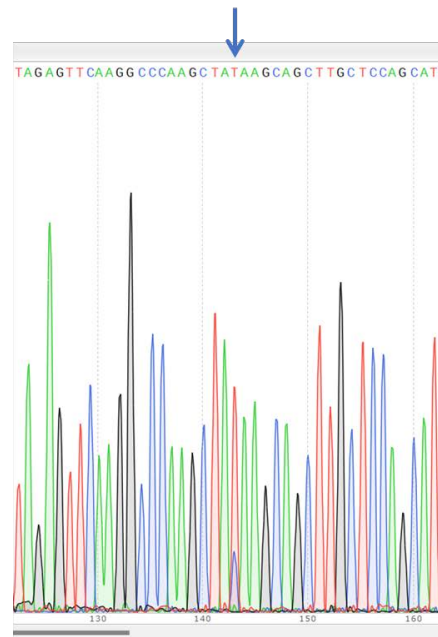
Sorted CD3+ T cell sample

c.751C>T



Diagnosis sample

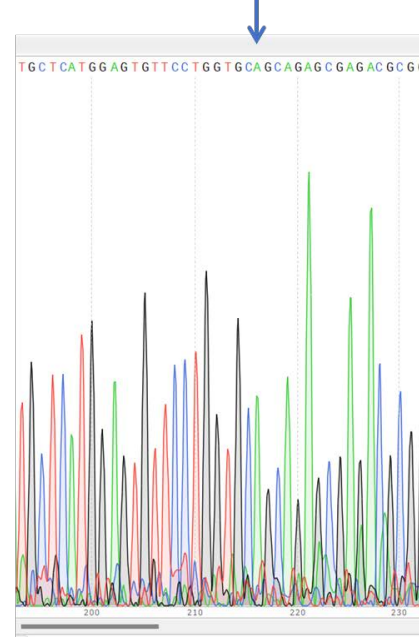
c.751C>T



UPN3436

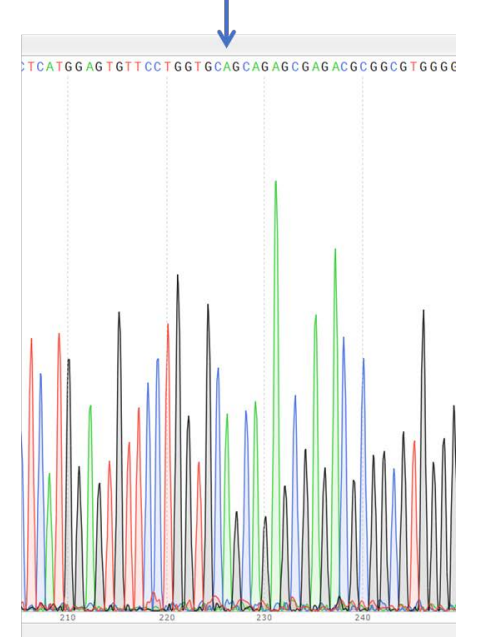
Buccal sample

c.1175G>A



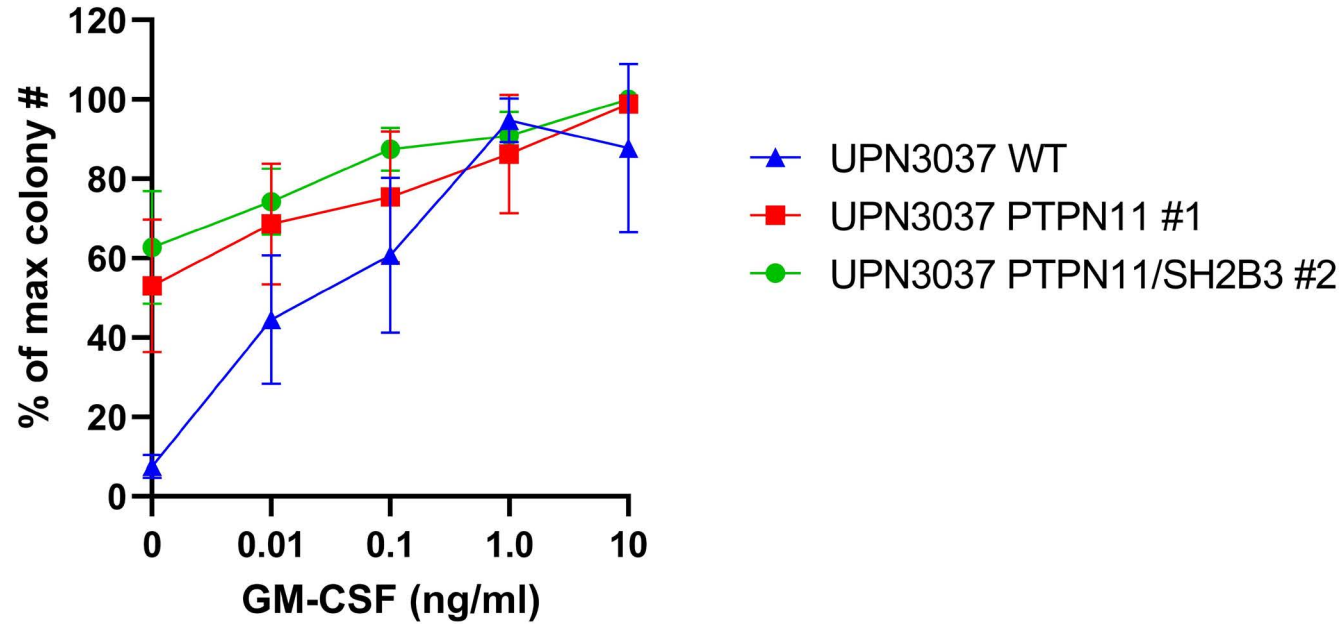
Diagnosis sample

c.1175G>A



A

CFU-GM assay HPC day 9/10

**B**